

Modification of a Specific Class of Plasmodesmata and Loss of Sucrose Export Ability in the *sucrose export defective1* Maize Mutant

William A. Russin,^{a,1} Ray F. Evert,^a Peter J. Vanderveer,^a Thomas D. Sharkey,^a and Steven P. Briggs^b

^a Department of Botany, University of Wisconsin, 430 Lincoln Drive, Madison, Wisconsin 53706

^b Pioneer Hi-Bred International, Inc., 7300 N.W. 62nd Avenue, Johnston, Iowa 50131

We report on the export capability and structural and ultrastructural characteristics of leaves of the *sucrose export defective1* (*sed1*; formerly called *sut1*) maize mutant. Whole-leaf autoradiography was combined with light and transmission electron microscopy to correlate leaf structure with differences in export capacity in both wild-type and *sed1* plants. Tips of *sed1* blades had abnormal accumulations of starch and anthocyanin and distorted vascular tissues in the minor veins, and they did not export sucrose. Bases of *sed1* blades were structurally identical to those of the wild type and did export sucrose. Electron microscopy revealed that only the plasmodesmata at the bundle sheath-vascular parenchyma cell interface in *sed1* minor veins were structurally modified. Aberrant plasmodesmal structure at this critical interface results in a symplastic interruption and a lack of phloem-loading capability. These results clarify the pathway followed by photosynthates, the pivotal role of the plasmodesmata at the bundle sheath-vascular parenchyma cell interface, and the role of the vascular parenchyma cells in phloem loading.

INTRODUCTION

Control of photosynthate export and carbon partitioning is complex (Geiger, 1979; Turgeon, 1989) and can be influenced by a range of factors, for example, growth stage of the plant (Eastin, 1969), source activity, sink strength, and the vascular connections between source leaves and nearby sinks (Wyse, 1986; Wardlaw, 1990). A critical step in supplying growing regions of the plant with reduced carbon is phloem loading in source leaves. Therefore, understanding the pathway of photosynthate transport and mechanisms of phloem loading is important for understanding carbon export, partitioning, and sink-to-source transition in leaves.

Two opposing routes are generally recognized both for pathways of photosynthate transport and for phloem loading in source leaves: symplastic and apoplastic. The great variation in source leaf structure and physiology suggests that neither route is universal (Delrot, 1987; van Bel, 1987, 1993; Turgeon, 1989; Turgeon and Beebe, 1991). Plasmodesmata play a prominent role in the symplastic transport of photoassimilates from the mesophyll to the region of the vascular bundle. In some species, they may play a direct role in the process of sieve tube loading (Turgeon, 1989; Beebe and Evert, 1992). Plasmodesmal frequency (e.g., Evert et al., 1977; Botha and Evert, 1988; Botha and van Bel, 1992; Evert and Russin, 1993) and developmental modifications in plasmodesmal structure and/or number (Ding et al., 1988; Beebe and Evert, 1992) may have

a strong influence on the mode and rate of phloem loading (van Bel, 1993).

Initially, plasmodesmata were thought to be simple structures that functioned mainly as passive channels (Lucas et al., 1993a; Epel, 1994). However, current evidence indicates that plasmodesmata are both structurally (Botha et al., 1993; Gamalei et al., 1994) and functionally complex. They play an integral role in the transport of a variety of substances, including nutrients and small signaling molecules (Oparka, 1993), as well as in the trafficking of various macromolecules (Lucas et al., 1993a, 1995; Epel, 1994; Waigmann and Zambryski, 1995). Plasmodesmata apparently transport substances selectively based on the size, charge, and structure of the transport molecule (Tucker and Tucker, 1993). Furthermore, plasmodesmal structure, composition, and regulation may differ in different cells and tissues (Robinson-Beers et al., 1990; Epel, 1994; Waigmann and Zambryski, 1995).

Maize is an excellent plant for studying sucrose transport and phloem loading because of its high rates of photosynthesis and sucrose export (Kalt-Torres et al., 1987) and our extensive knowledge of its vasculature and ultrastructure (Evert et al., 1977, 1978, 1985, 1996; Russell and Evert, 1985; Evert and Russin, 1993; Bosabalidis et al., 1994). In the maize leaf (Fritz et al., 1989) and in wheat leaves (Altus and Canny, 1982), there is a division of labor among vein orders. The major veins function mostly in the long-distance transport of photosynthate out of the source leaf and into the sink organ. In contrast, minor veins are mostly involved with loading photosynthate from

¹ To whom correspondence should be addressed.

surrounding mesophyll. The data available on phloem loading in the maize leaf indicate that photosynthates most likely follow a symplastic pathway from mesophyll cells to the bundle sheath cells and that the sieve tubes are loaded apoplastically (Evert, 1986). In minor veins of the maize leaf, the vascular parenchyma cells occupy most of the interface between the bundle sheath and sieve tubes (Evert, 1986). Because of this close spatial association, the vascular parenchyma cells probably are the first cells of the vascular tissue to receive photosynthate from the bundle sheath cells (Evert, 1986).

Numerous experimental methods have been used to study the control of carbon partitioning and the mechanism of phloem loading. These methods include mechanical manipulations of source or sink (e.g., Allison and Weinmann, 1970; Thiagarajah et al., 1981; Tollenaar and Daynard, 1982) and use of proton-sucrose symport-inhibiting compounds (e.g., Heyser, 1980; Bourquin et al., 1990). Dye transport studies have been used to determine the extent of symplastic continuity (Madore et al., 1986; van Bel et al., 1988) and the size exclusion limit and selectivity of plasmodesmal transport (Tucker, 1993; Tucker and Tucker, 1993).

Recently, molecular techniques using transgenic plants have yielded a great deal of information on the involvement of sucrose carrier protein in phloem loading (Bush, 1993; Reismeyer et al., 1992, 1993, 1994), on sink-source relations (Sonnewald et al., 1994), and on the metabolism and compartmentation of carbohydrates (Stitt and Sonnewald, 1995). Similar techniques have been applied to studies of plasmodesmal function. These studies have used both the transgenic plant approach (Wolf et al., 1989; Moore et al., 1992; Ding et al., 1993; Lucas et al., 1993b) and microinjection of viral movement proteins (Waigmann and Zambryski, 1994, 1995) to modify plasmodesmal structure. Transgenic tobacco plants have been used to study the influence of the tobacco mosaic virus movement protein (TMV MP) on carbon metabolism and photosynthate partitioning (Lucas et al., 1993b).

Identification and characterization of naturally occurring mutants have long been important methods for gaining insight into biological processes (Koch et al., 1982; Nelson and Pan, 1995). Numerous maize mutants have been identified. Some of these have been used to study developmental and physiological processes, such as *bundle sheath defective* (Langdale and Kidner, 1994) and the *KNOTTED* family of genes (Jackson et al., 1994; Lucas et al., 1995). Use of mutant varieties to study transport phenomena has some potential advantages over the previously mentioned methods: (1) experimental alteration does not involve invasive and possibly injurious procedures, and (2) no inhibitors with potential secondary effects are necessary (Koch et al., 1982; van Bel, 1993). The limitation to this method is the identification and characterization of a mutant variety that is appropriate for the given study.

A naturally occurring maize mutant has been identified with characteristics that indicate a reduced capacity for sucrose transport (S.P. Briggs, unpublished data). In plants exhibiting

the mutant phenotype, overall height was reduced by 25 to 50% (Figure 1A). As leaves developed, anthocyanin accumulated in a nonclonal pattern soon after leaves had emerged from the sheaths of older encircling ones. The appearance of anthocyanin began at the tip of the leaf and then progressed basipetally and laterally toward the margins (Figures 1B and 1C). Basipetal progression of anthocyanin rarely, if ever, extended fully to the base of the lamina (Figures 1A and 1B). The mutant leaves contained a higher than normal level of sugar (S.P. Briggs, unpublished data).

This maize mutant was originally named *sucrose transport1*, with the abbreviation *sut1* (Neuffer et al., 1996). However, several well-characterized sucrose transporter genes also have been named *sut* (e.g., Reismeyer et al., 1992, 1993, 1994). Because we have no evidence that this maize mutation is directly related to a sucrose transporter gene, we have chosen to rename our mutant *sucrose export defective1* (*sed1*) to avoid possible confusion.

We report on the export capability and structural and ultrastructural characteristics of leaves of the *sed1* maize mutant. Transport patterns were studied by feeding $^{14}\text{CO}_2$ to source leaves of both wild-type plants and *sed1* mutants and then by assessing their capacity for exporting photosynthate. We correlated these transport characteristics with structural differences in the *sed1* plants by using light and electron microscopy. The *sed1* mutation appears to affect a critical interface of minor veins. This characteristic allowed us to investigate the importance of this class of plasmodesmata in sucrose export and presumably phloem loading.

RESULTS

Transport of Labeled Carbon

Blades of wild-type plants used in the labeling studies lacked abundant anthocyanin (Figure 1C). Feeding $^{14}\text{CO}_2$ to the tip of a source leaf (either leaf 1 [L1] or leaf 3 [L3]) of the wild-type plants resulted in labeled carbon being fixed in the fed region. Labeled photosynthate was subsequently exported to sink regions in both shoots and roots (Figures 2A and 2B). Autoradiography of wild-type plants in which the tip of L1 was fed showed that labeled photosynthate was transported to the base of L3 and L4, most of L5, and the roots (Figure 2A). A similar distribution of label was obtained when the tip of L3 of a wild-type plant was fed. Labeled photosynthate was exported from the tip of L3 and distributed to the sheath of L3, the base of L4, the entirety of L5, and the roots (Figure 2B).

In the *sed1* plants, the leaf tips that were fed had abundant anthocyanin (Figure 1C). As in wild-type plants, when $^{14}\text{CO}_2$ was fed to the tip of L1 or L3 in *sed1* plants, labeled carbon was fixed in the fed area (Figures 2C and 2D). However, autoradiography of the *sed1* plants showed that the label remained confined mostly to the region that was fed. Unlike wild-type

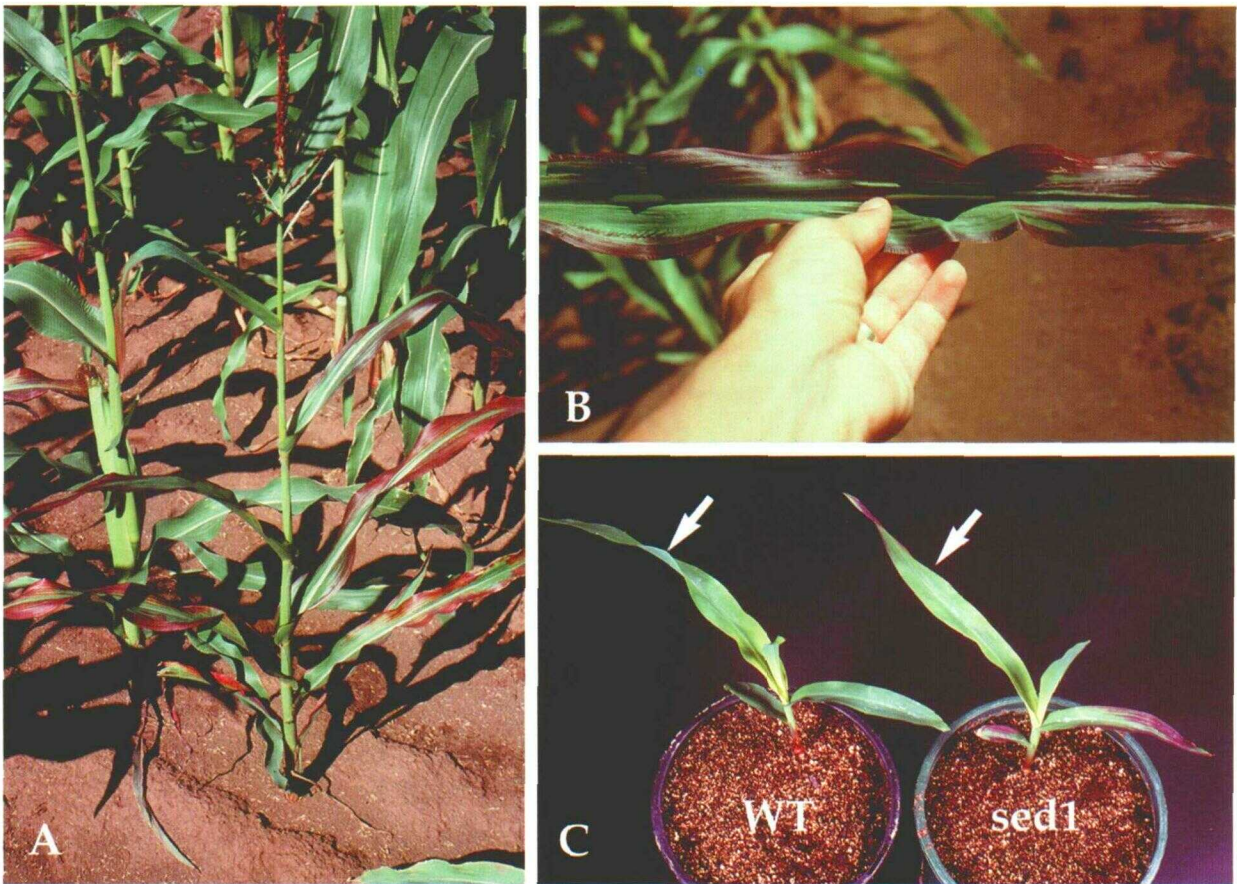


Figure 1. *sed1* Plants.

(A) *sed1* plant in a field plot showing reduced overall plant stature, abundant anthocyanin, and tassel.

(B) Fully expanded field-grown *sed1* leaf showing obvious anthocyanin along leaf margin (tip of leaf toward right).

(C) Plants at the growth stage used in this study. L3 (arrow) of a wild-type (WT) plant at left shows normal pigmentation. L3 (arrow) of a *sed1* plant has conspicuous anthocyanin.

plants, no label was found in sink regions in the *sed1* plants (Figures 2C and 2D). Nearly identical results were obtained for L1 or L3.

Liquid scintillation counting of leaf samples confirmed that a substantial amount of carbon was fixed in the fed regions of both wild-type and *sed1* plants. Samples taken from within the regions that were fed (both L1 and L3) from both wild-type and *sed1* leaves showed appreciable amounts of radioactivity (Table 1). However, there were large differences in radioactivity from sink leaves of *sed1* plants when compared with that in similar samples of wild-type plants. A substantial amount of ^{14}C was present in samples taken from sink leaves of wild-type plants, regardless of which leaf was fed (Table 1). In contrast, comparable samples taken from sink leaves of *sed1* plants contained very little labeled photosynthate (Table 1). Sink leaves of *sed1* plants in which L1 was fed contained approximately

one-tenth the label of sink leaves of wild-type plants (Table 1). In contrast, sink leaves of *sed1* plants in which L3 was fed contained almost no ^{14}C (Table 1).

Examination of the x-ray films revealed that the fleshy roots had stuck to and damaged the photographic emulsion, compromising our interpretation (Figures 2A to 2D). Data from liquid scintillation counts, however, showed that the roots of *sed1* plants had at most 5% of the amount of ^{14}C present in roots of wild-type plants. The data were similar regardless of which leaf was fed (Table 1). The combined results of autoradiography and liquid scintillation counting indicate that carbon was fixed in the tips of source leaves of *sed1* plants, but virtually none of that carbon was exported to any sink region.

Fully expanded L3 blades from *sed1* plants had abundant anthocyanin at the tips but lacked anthocyanin at the base. The lamina base of L3 from a *sed1* plant looked similar to the

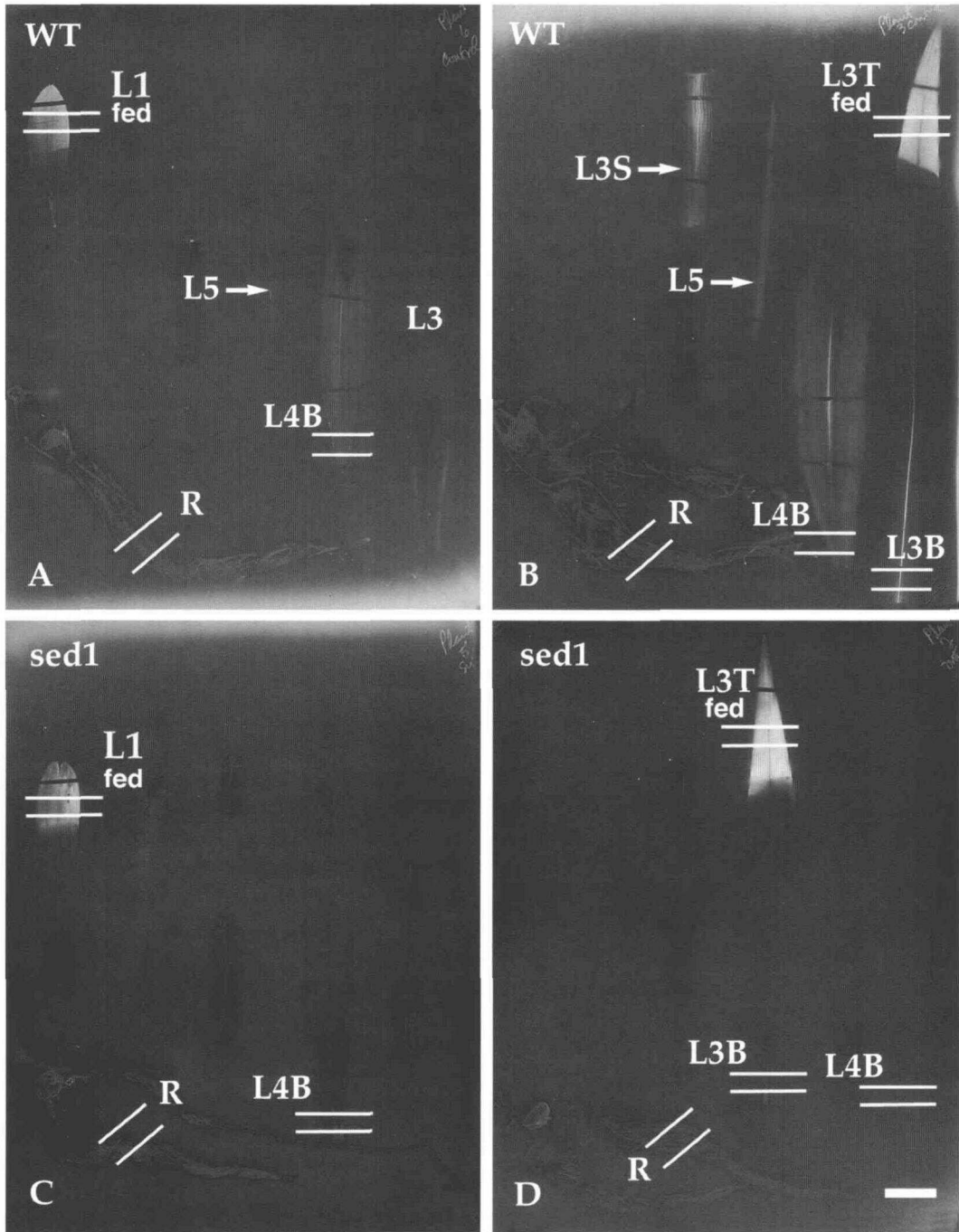


Figure 2. Autoradiography of Wild-Type and *sed1* Plants That Were Fed $^{14}\text{CO}_2$.

Wild-type (WT) plants export labeled photosynthate from the fed areas (A) and (B), whereas *sed1* plants do not export labeled photosynthate (C) and (D). White lines indicate areas sampled for scintillation counts. B, base of lamina; R, roots; S, sheath; T, tip of lamina.

(A) Wild-type plant: L1 fed area.

(B) Wild-type plant: L3 fed area.

(C) *sed1* plant: L1 fed area.

(D) *sed1* plant: L3 fed area.

Bar in (D) for (A) to (D) = 10 mm.

Table 1. Amount of Labeled Photosynthate Contained in Different Portions of Both Wild-Type and *sed1* Plants^a

Sample Position ^b	WT (dpm) ^c	<i>sed1</i> (dpm)
L1 tip (fed)	6,259	7,636
L4 base	3,445	407
Root	5,847	300
L3 tip (fed)	7,297	12,666
L3 base	3,039	108
L4 base	5,373	19
Root	6,924	84

^a The amount of labeled photosynthate was determined by liquid scintillation counting.

^b Sample positions are indicated in Figures 2A to 2D.

^c The average background radiation during scintillation counting was 69.4 ± 45.8 dpm; this value was determined by counting blanks containing only scintillation cocktail. WT, wild type.

lamina base of L3 from wild-type plants. We fed ¹⁴CO₂ to the basal region of the blade of L3 on a *sed1* plant to determine whether this region could export photosynthate. Autoradiography with L3 lamina in which the base was fed showed heavy label throughout the fed region, indicating that carbon was being fixed (Figure 3). Abundant label also was found in the sheath below the fed region (Figure 3), providing evidence that radioactive photosynthate is exported from the normal-appearing lamina base of a *sed1* leaf. These results demonstrate that the normal appearance of the *sed1* leaf base is correlated with export competence, whereas the aberrant appearance of the *sed1* leaf tip is correlated with a lack of export competence.

Description of Leaf Structure

The arrangement of tissues in the lamina of both wild-type (Figures 4A, 4C, and 4E) and *sed1* (Figures 4B, 4D, and 4F) leaves is similar to that described for other maize cultivars (e.g., Evert et al., 1977, 1978; Russell and Evert, 1985). Maize leaves have the anatomy typical of a C₄ NADP-malic enzyme-type species: mesophyll cells radially arranged around a chlorenchymatous bundle sheath that, in turn, surrounds the vascular tissue (Evert et al., 1977). Three orders of longitudinal vascular bundle can be recognized in the maize leaf: large, intermediate, and small. For the purposes of this study, however, the longitudinal veins are referred to simply as either major or minor (Bosabalidis et al., 1994). Major veins (large) are characterized by the presence of large metaxylem vessels on either side of protoxylem or a protoxylem lacuna and by the presence of both protophloem and metaphloem. Minor veins (intermediate and small) lack large metaxylem vessels and protoxylem, and in most, the phloem consists entirely of metaphloem (Russell and Evert, 1985).

Light microscopic examination of transverse leaf blade sections showed that wild-type leaves, regardless of sampling region, had a structure consistent with that reported for other maize leaves (described above). The size and distribution of mesophyll and bundle sheath cells in wild-type leaves are consistent with previous reports (Figures 4A, 4C, and 4E). The mesophyll cell chloroplasts contained few small starch grains, whereas the bundle sheath cell chloroplasts contained numerous large starch grains (Figures 4A, 4C, and 4E). All vein orders from all sampling regions of wild-type leaves had a structure typical of that found in other maize leaves.

At the tip of *sed1* blades, the mesophyll cells and bundle sheath cells were somewhat enlarged and distorted (Figure 4B). Starch grains were abnormally large and abundant in both the mesophyll cell chloroplasts and bundle sheath cell chloroplasts (Figure 4B). In addition, starch grains appeared to be equally abundant in both the mesophyll and bundle sheath

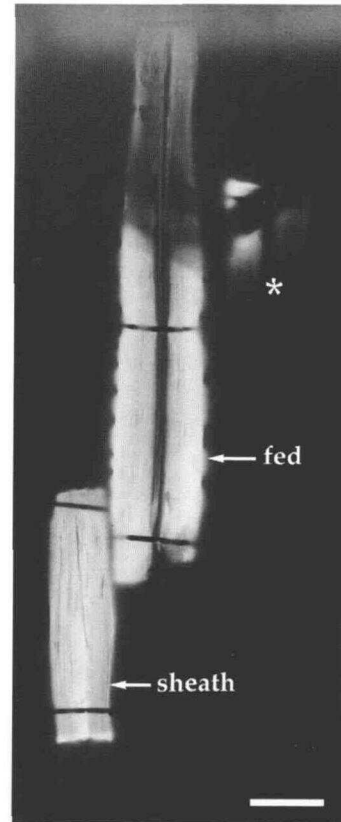


Figure 3. Autoradiography of *sed1* L3 Lamina Base.

A normal-appearing lamina base of a *sed1* plant was fed labeled carbon (fed, at arrow), and labeled photosynthate was subsequently exported through the sheath (sheath, at arrow). The asterisk indicates a small portion of the fed region where L3 was cut to fit on x-ray film. Bar = 20 mm.

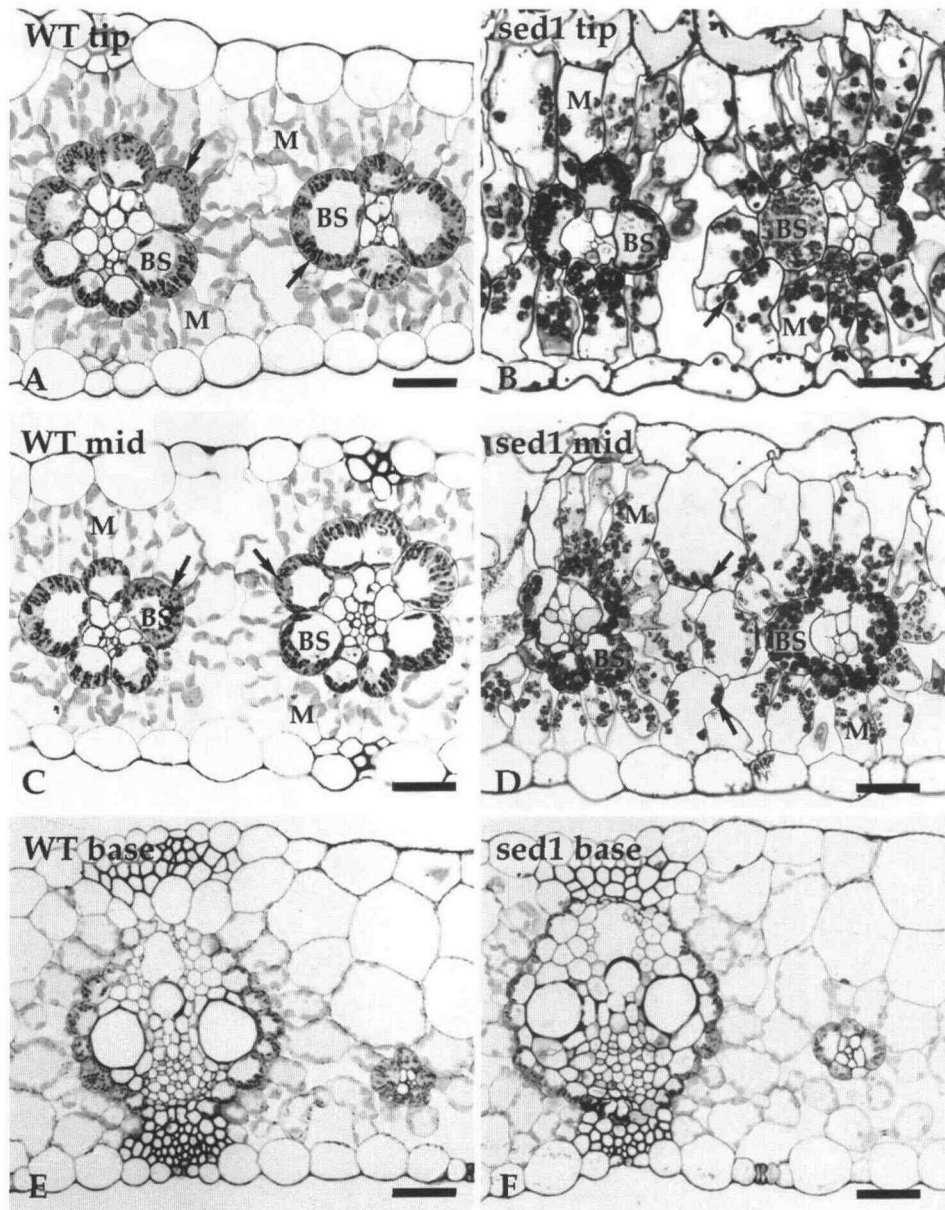


Figure 4. Light Microscopy of Transverse Sections from the Three Sampling Regions of Both Wild-Type and *sed1* Blades.

The wild-type (WT) blades in (A), (C), and (E) show mesophyll cells (M) radially arranged around the large bundle sheath cells (BS). Wild-type blades in (A), (C), and (E) show abundant starch accumulation in the bundle sheath cells (arrows in [A] and [C]), but virtually no starch in mesophyll cells. *sed1* blades are structurally similar to those of the wild type. The mesophyll cells and bundle sheath cells at the tip of the *sed1* lamina appear distended. Abundant starch is found in the mesophyll (arrows) and bundle sheath cells at the lamina tip of *sed1* leaves (B). The mid-region samples of *sed1* blades in (D) have abundant starch in the bundle sheath cells but less in the mesophyll cells (arrows) compared with the tip. The bases of wild-type (E) and *sed1* (F) blades are virtually identical structurally.

(A) Wild-type tip.

(B) *sed1* tip.

(C) Wild-type mid-region (mid).

(D) *sed1* mid-region.

(E) Wild-type base.

(F) *sed1* base.

Bars in (A) to (F) = 10 μm .

cells (Figure 4B). In the mid-region of the lamina, mesophyll and bundle sheath cells were still enlarged and distorted. However, starch grains were smaller and less abundant in the mesophyll than in the bundle sheath (cf. Figures 4C and 4D). Structurally, the base of the *sed1* lamina was virtually indistinguishable from the base of the wild-type lamina (cf. Figures 4E and 4F).

The vascular tissues of *sed1* leaves also were structurally modified. These modifications were expressed differentially, depending on both sampling region and type of vein. No perceptible differences were detected in the vascular tissue of the major veins of either wild-type or *sed1* plants, regardless of sampling region (Figures 4E and 4F, base; Figures 5A and 5B, tip). In the minor veins at the tip of *sed1* blades, however, there were conspicuous modifications to the vascular tissues. The vascular parenchyma cells that abut the bundle sheath cells were greatly enlarged and distorted, and they appeared to be plasmolyzed (Figure 5D). At the mid-region of the lamina, the minor veins were less distorted than minor veins at the tip, but the vascular parenchyma cells still appeared to be plasmolyzed (Figure 5E). Minor veins from the basal region of *sed1* blades were virtually identical with those found in wild-type leaves (cf. Figures 5C and 5F). Therefore, the overall expression of the *sed1*-conferred phenotype is greatest at the tip of the lamina and least at the base. In addition, the expression of *sed1* in the vascular tissue is restricted almost exclusively to the minor (small and intermediate) veins.

Plasmolysis of the vascular parenchyma cells in minor veins of the *sed1* lamina tip is not a fixation artifact. There was no evidence of plasmolysis in vascular parenchyma cells of major veins from the sampling region. In addition, no plasmolysis was observed in any of the cells from wild-type tissues.

Ultrastructure of Plasmodesmata

Previous studies indicate that, in maize, photosynthates most likely follow a symplastic pathway from mesophyll cells to the vascular parenchyma cells (Evert et al., 1977; Evert and Russin, 1993). To determine whether the characteristics of *sed1* plants might include a symplastic interruption or block, we examined plasmodesmata at pertinent cell interfaces, from mesophyll to phloem, in both wild-type and *sed1* leaves. This examination was restricted to the tip and basal lamina regions to obtain a clear-cut comparison of plasmodesmal structure between a region shown to be incapable of export (*sed1* tip) and a region that is capable (*sed1* base).

The plasmodesmal structures observed at all interfaces in wild-type leaves were consistent with previous descriptions (Evert et al., 1977) (Figures 6A, 6C, and 6E). In samples from the tip of *sed1* leaves, plasmodesmata at the mesophyll cell–mesophyll cell, bundle sheath cell–bundle sheath cell (not shown), and mesophyll cell–bundle sheath cell (Figure 6B) interfaces were similar in appearance to those of the wild type. The only interface at which the plasmodesmata differed

between the wild type and *sed1* was at the bundle sheath–vascular parenchyma cell (BS-VP) interface of minor veins (Figure 6D). The plasmodesmata on the bundle sheath cell side of the interface appeared contorted and discontinuous. Examination of serial sections showed that in most cases, the plasmodesmata were completely covered by a layer of wall material through which they did not extend. At the base of the *sed1* leaf, all plasmodesmata, including those at the BS-VP interface, appeared identical to those of the wild type (cf. Figures 6E and 6F).

There is evidence that the observed plasmodesmal modification is quite specific to the BS-VP interface of the minor veins. First, within a single bundle sheath cell of a minor vein, normal plasmodesmal structure has been observed at the bundle sheath cell–mesophyll cell and bundle sheath cell–bundle sheath cell interfaces. In the same cell, the plasmodesmata at the BS-VP interface had aberrant structure. Second, the plasmodesmata at the BS-VP interface in major veins at the tip of *sed1* leaves were apparently unmodified (Figure 7).

DISCUSSION

We found that tips of *sed1* leaves did not export photosynthate and had modified plasmodesmal structure at the BS-VP interface. The structural modifications observed at the light microscope level in *sed1* plants were not expressed uniformly throughout the leaf; we found a strong tip-to-base gradient. Accumulation of anthocyanin and starch as well as structural abnormalities in the vascular tissues of minor veins were most prominent at the tip of the lamina, with a gradual decline toward the base. The structurally modified *sed1* lamina tips apparently do not export photosynthate. The small amount of labeled photosynthate detected by liquid scintillation counting in the *sed1* sink regions (plants in which L1 was fed) could be accounted for. It is possible that major veins in L1 have a limited ability to load photosynthate. In contrast to the tip, the structurally unmodified lamina base of *sed1* leaves apparently exports photosynthate. Determination of a continuous gradient of plasmodesmal modifications was beyond the scope of this article. We did find, however, that the only modified plasmodesmata occurred at the BS-VP interface at the tip of *sed1* leaves. At the base of the *sed1* lamina, all plasmodesmata were similar in structure to those in the wild type. Therefore, our results demonstrate a strong correlation between structural features and export competence in the *sed1* leaves.

Maize leaves normally export ~80% of assimilated carbon as sucrose, whereas ~15% is incorporated into starch (Kalt-Torres et al., 1987; Rocher, 1988). In fact, under most conditions, maize leaves accumulate starch in bundle sheath cell chloroplasts but not in mesophyll cell chloroplasts (Rhoads and Carvalho, 1944; Downton and Hawker, 1973). Low starch accumulation in wild-type maize leaves has been attributed

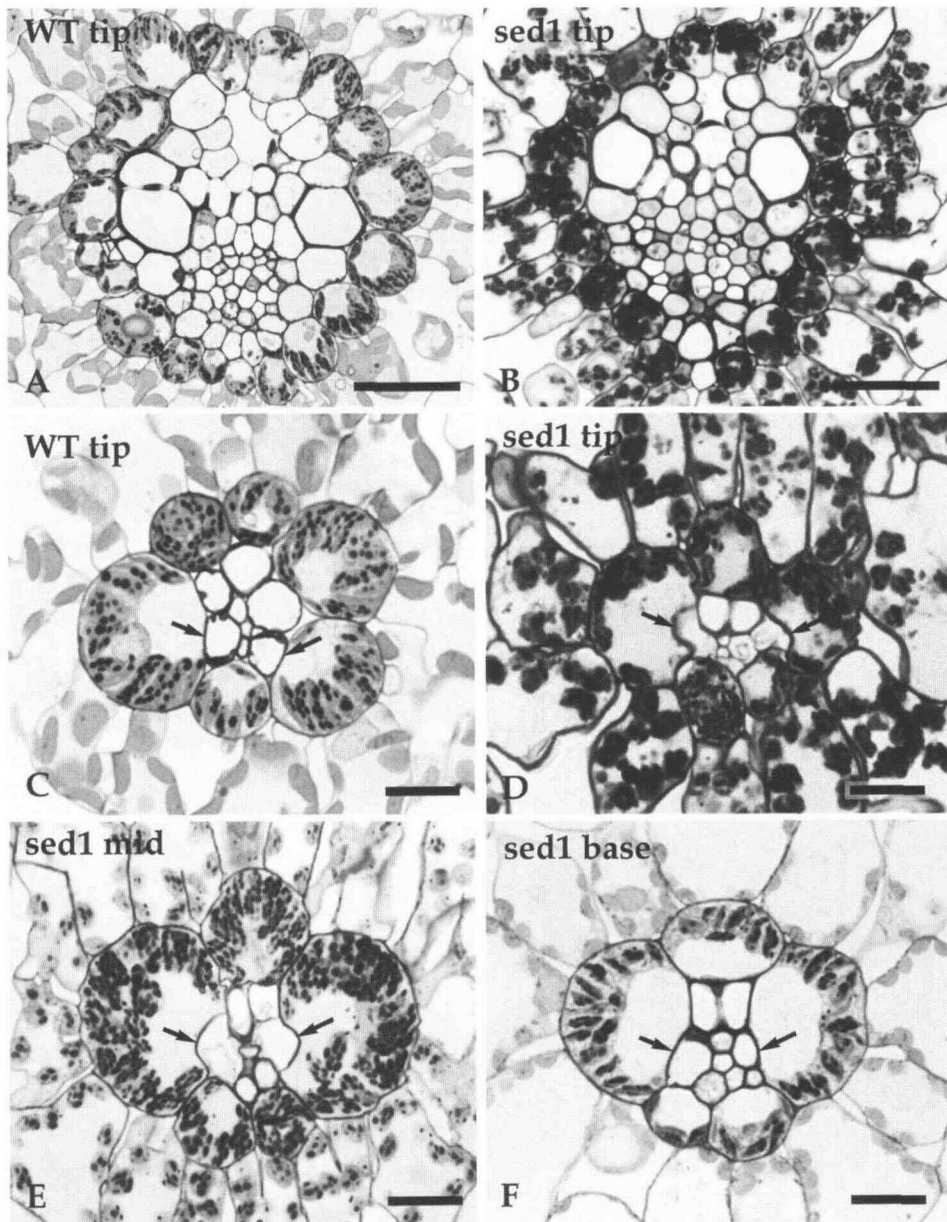


Figure 5. Light Microscopy of Representative Major and Minor Veins from Both Wild-Type and *sed1* Blades.

The vascular tissues are similar in major veins at the tip of wild-type (WT) (A) and *sed1* (B) blades. Compared with the vascular tissues of minor veins at the lamina tip of wild-type leaves (C), those of minor veins at the lamina tip of *sed1* leaves (D) are strongly affected. The vascular parenchyma cells (arrows) are conspicuously distorted and appear plasmolyzed. The deformed vascular parenchyma cells are less apparent in mid-region samples (arrows in [E]). Finally, at the base of the *sed1* blade, the minor veins are comparable structurally with minor veins of the wild-type (cf. [C] and [F]).

(A) Major vein in a wild-type tip.

(B) Major vein in a *sed1* tip.

(C) Minor vein in a wild-type tip.

(D) Minor vein in a *sed1* tip.

(E) Minor vein in a *sed1* mid-region (mid).

(F) Minor vein in a *sed1* base.

Bars in (A) and (B) = 10 μm ; bars in (C) to (F) = 5 μm .

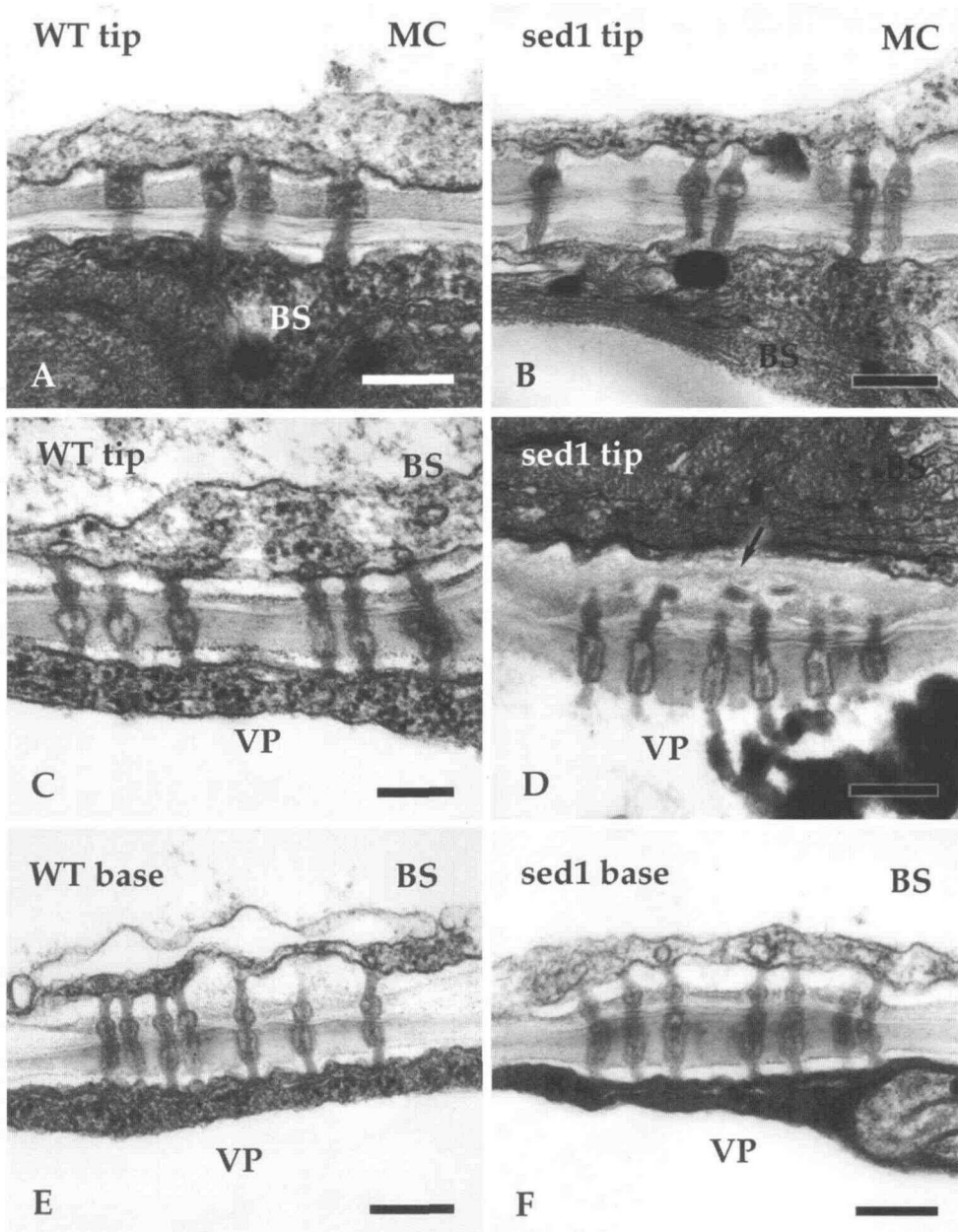


Figure 6. Transmission Electron Microscopy of Plasmodesmata along the Symplastic Pathway from Mesophyll Cell to Bundle Sheath and Vascular Parenchyma Cells in Both Wild-Type and *sed1* Blades.

The structure of plasmodesmata at the mesophyll cell–bundle sheath cell (MC–BS) interface is similar in tip samples of both wild-type (WT) (A) and *sed1* (B) blades. Compared with the wild-type structure at the BS–VP interface in tip samples (C), the plasmodesmata at the BS–VP interface in minor veins of the *sed1* lamina tip (D) are greatly distorted and covered by cell wall material (arrow). In contrast, the plasmodesmata at the BS–VP interface of minor veins at the base of both wild-type (E) and *sed1* (F) blades are structurally similar.

- (A) Wild-type lamina tip at the MC–BS interface.
- (B) *sed1* lamina tip at the MC–BS interface.
- (C) Wild-type lamina tip at the BS–VP interface.
- (D) *sed1* lamina tip at the BS–VP interface.
- (E) Wild-type lamina base at the BS–VP interface.
- (F) *sed1* lamina base at the BS–VP interface.

Bars in (A) to (F) = 200 nm.

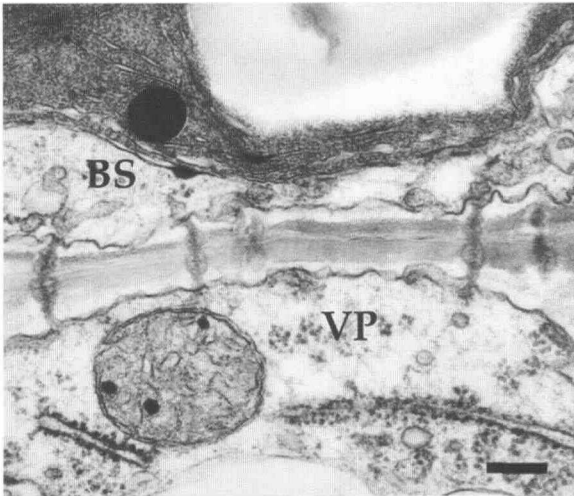


Figure 7. Transmission Electron Microscopy of Plasmodesmata at an Interface in a Major Vein at the Tip of a *sed1* Lamina.

This interface is the equivalent of the BS-VP interface in a minor vein. Bar = 200 nm.

to high export rates (Kalt-Torres et al., 1987) and the proximity of active sinks (Koch et al., 1982).

In studies in which the balanced source–sink ratio of maize plants is experimentally disturbed, the plants apparently compensate through changes in carbohydrate partitioning (Tollenaar and Daynard, 1982). For example, the upper leaves of maize plants from which developing ears had been removed contained more than twice as much sugar and three times as much starch as in leaves of control plants (Allison and Weinmann, 1970). The elevated sucrose concentration in such areas would most likely affect starch accumulation (Geiger, 1979). Soluble sugars are converted into starch in bundle sheath cells when the rate of sugar movement into the bundle sheath cells is greater than the rate of transport into the vascular tissue (Rhoads and Carvalho, 1944). Maize leaves accumulate starch in mesophyll cells when treated with sugar solution (~ 0.3 M) (Rhoads and Carvalho, 1944; Kutik and Beneš, 1981) or when exposed to continuous illumination (Downton and Hawker, 1973). In addition to starch, anthocyanin accumulates in maize leaves when sugar concentrations are abnormally high, such as when a major sink is absent or removed (Allison and Weinmann, 1970; Thiagarajah et al., 1981; Tollenaar and Daynard, 1982). We predict that (1) the accumulation of starch and anthocyanin observed in *sed1* leaves is likely to be caused by abnormally high sucrose concentrations, and (2) the structural modifications seen in the vascular tissues at the tip of *sed1* leaves had an effect similar to that of mechanical sink removal by preventing movement of photosynthates into vascular parenchyma cells and hence the sieve tubes of minor veins.

We have demonstrated differential expression of *sed1* based on vein order. The vascular tissues of the major veins appear

structurally unaltered in all areas of the *sed1* lamina. These veins are the first to be initiated and to mature (Evert et al., 1978; Russell and Evert, 1985; Evert and Russin, 1993). Also, all major veins in the maize leaf are continuous with the stem vasculature (Russell and Evert, 1985). In contrast, the vascular tissues of the minor veins in the tip and mid-leaf regions of *sed1* leaves are strongly affected. Minor veins are initiated later in leaf development and differentiate basipetally. The vast majority of the minor veins ultimately fuse with adjacent veins above or in the region of the blade joint (Russell and Evert, 1985). These structural characteristics, in combination with results of autoradiographic studies (Pristupa, 1964; Hofstra and Nelson, 1969; Fritz et al., 1989), indicate a specificity of function for the different vein orders. Major veins function primarily in long-distance transport of photosynthate both into immature, importing (sink) leaves and out of mature, exporting (source) leaves. Minor veins in the maize leaf are concerned primarily with loading of photosynthate from the mesophyll and shunting it to the large veins for export. Considering that the major (transport) veins of *sed1* leaves are unperturbed and the minor (loading) veins are strongly perturbed, we conclude that the *sed1* mutation probably affects phloem loading rather than long-distance transport.

Visual inspection of growing *sed1* leaves indicates that they develop normally up to a point that correlates loosely with the initiation of sink-to-source transition (W.A. Russin and R.F. Evert, unpublished data). Results from a recent autoradiographic study have shown that regions of maize leaves stop importing at approximately the time they become unensheathed or exposed (Evert et al., 1996). Because the effects of the *sed1* mutation are specific to vein order, it is possible that the timing of vascular initiation/maturation may play a role in development of the mutant phenotype. Cessation of photosynthate import associated with sink-to-source transition has been correlated with closure or alteration of plasmodesmata along the symplastic pathway (Turgeon, 1989; Beebe and Evert, 1992) and with a decrease in plasmodesmal frequencies during the transition of the leaf tissue from an importing to a nonimporting state (Ding et al., 1988). The lack of export competence in *sed1* plants may be a gradual process resulting from progressive modification of plasmodesmal structure, perhaps because of a pressure-mediated closure of plasmodesmata (Oparka and Prior, 1992). Alternatively, the plasmodesmata at the BS-VP interface simply might never develop correctly. In that case, the gradual onset of the *sed1*-conferred phenotype indicates that plasmodesmata may play different roles during the importing and exporting phases of leaf development.

In maize leaves, there are considerable numbers of plasmodesmata in the walls between mesophyll and bundle sheath cells (Evert et al., 1977). In addition, the continuous, impermeable suberin lamellae in the outer tangential and radial walls of the bundle sheath cells (Hattersley and Browning, 1981; Evert et al., 1985) act as effective barriers to movement of apoplastic solutes (Heyser, 1980; Evert et al., 1985). At the inner tangential wall, suberin lamellae are found only at the site of

plasmodesmal connections to vascular parenchyma cells. Although the compound middle lamella of the radial walls of the bundle sheath cells may serve as an apoplastic pathway from vascular bundle to mesophyll (Evert et al., 1985), it is likely to be a minor route at best. Therefore, the major transport pathway of primary assimilates between the mesophyll and bundle sheath cells must be symplastic (Heyser, 1980; Evert, 1986).

Current evidence indicates that phloem loading (and unloading) in the maize leaf is apoplastic (Heyser, 1980; Evert, 1986; Evert and Russin, 1993). The BS-VP interface contains numerous plasmodesmata but lacks suberin lamellae, except in the region containing plasmodesmata. Because the inner tangential wall of the bundle sheath cells is mostly nonsuberized, the potential exists for photosynthate to exit the symplast from either the bundle sheath cells or the vascular parenchyma cells. Because of the high plasmodesmal frequency at the BS-VP interface, transport of sucrose from bundle sheath cells to the vascular parenchyma cells in minor veins could be either apoplastic or symplastic (Evert et al., 1978).

Our results help to clarify the pathway of photosynthetic metabolites from the mesophyll to the vascular tissues. Disruption of plasmodesmal connections and, hence, symplastic continuity at the BS-VP interface in *sed1* plants appear to block the loading of photosynthates. The plasmodesmata at the BS-VP interface apparently are critical in the transfer of photosynthate from bundle sheath cells to vascular tissue. Therefore, it is likely that the vascular parenchyma cells, not the bundle sheath cells, mediate the entry of photosynthate into the apoplast for loading into the sieve tube–companion cell complexes. Vascular parenchyma cells in the maize leaf are not symplastically isolated, however, from thick-walled sieve tubes or from other vascular parenchyma cells (Evert et al., 1977; Evert and Russin, 1993). Although the vascular parenchyma cells were severely plasmolyzed, plasmodesmata at the other interfaces (except at the BS-VP interface) appeared structurally normal. From this evidence, we conclude that photosynthates most likely follow a symplastic route from the mesophyll to the vascular parenchyma cells. The vascular parenchyma cells then unload photosynthates into the apoplast, from which they are loaded into the sieve tube–companion cell complexes.

It is tempting to postulate that the *sed1* gene directly controls plasmodesmal development; however, recent work with transgenic tobacco plants suggests otherwise. Plasmodesmal structure has been modified by expression of genes as diverse as yeast acid invertase (Ding et al., 1993) and TMV MP (Wolf et al., 1989; Ding et al., 1992; Moore et al., 1992). Although the *sed1* mutation itself may directly affect some process other than plasmodesmal development (such as cell wall deposition or production of a signaling molecule), we believe that information gained from the *sed1* plants will be useful in the unraveling of plasmodesmal function and development. There are striking parallels between the effects of *sed1* and those produced by the 30-kD TMV MP in tobacco (Lucas et al., 1993b). The TMV MP apparently modifies plasmodesmal structures, thereby increasing their size exclusion limit (Ding et al., 1992). L5 and L6 of transgenic tobacco plants expressing TMV MP had a

higher than normal level of sugars (sucrose, glucose, and fructose) and an increased quantity of starch (Lucas et al., 1993b). Structurally modified plasmodesmata have been found at the mesophyll cell interfaces with other mesophyll cells, with epidermal cells, and with bundle sheath cells. However, the plasmodesmata at the BS-VP interface were unaltered, even though the protein is present in these plasmodesmata (Ding et al., 1992). Our results lend support to the suggestion that the plasmodesmata at the BS-VP interface are in some way unique and that they may play a pivotal role in a variety of processes (Ding et al., 1992; Leisner and Turgeon, 1993; Lucas et al., 1993b).

We recognize that physical disruption of plasmodesmal connections does not necessarily lead to cessation of plasmodesmal transport. For example, vascular bundle strands have been mechanically isolated from several C₄ grasses (including maize). The plasmodesmata of these isolated strands have been physically separated from the surrounding tissues, yet they apparently are still capable of transport (Burnell, 1988; Weiner et al., 1988; Valle et al., 1989). However, in *sed1* plants, the plasmodesmata are not only contorted and discontinuous but are also covered by a layer of cell wall material. This imposes an additional physical barrier between bundle sheath cells and vascular parenchyma cells. Currently, we are addressing these issues in a series of dye-coupling experiments and a determination of the nature of the occluding cell wall material.

Considering this evidence, we suggest the following hypothetical scheme of development for the *sed1*-conferred phenotype. Initially, sink leaves develop normally because the major (importing) vein structure is unaffected by the *sed1* mutation. Aberrant plasmodesmal structure at the BS-VP interface in minor veins imposes a structural interruption in the symplast, thereby preventing sucrose transport and subsequent loading and export from the leaf tip. Carbon continues to be fixed, but photosynthate cannot be exported. Sucrose (and possibly other intermediates) accumulates in the mesophyll and bundle sheath cells. Elevated sucrose concentrations in these cells leads to abnormal starch accumulation and distended cells. Osmotic stress causes the cells to accumulate anthocyanin.

METHODS

Plant Material

All plants used were from a non-inbred line of *Zea mays* ssp *mays* segregating for *sed1* (Pioneer Hi-Bred International, Johnston, IA). Seeds were planted in flats filled with vermiculite. After germination, the seedlings were transplanted to plastic pots filled with Metro-Mix that was mixed with Osmocote 14-14-14 pellets (Grace-Sierra Horticultural Products Co., Milpitas, CA) and grown in a greenhouse with supplemental light. Leaf numbers were assigned from the base of the plant. Once the plants reached 20 to 25 cm and the fourth leaf (L4) was extended >5 cm above the sheath (~2 weeks old), they were sorted into wild-type (control) and mutant (*sed1*) classes. Plants were assigned to the *sed1* category based on the persistent presence of anthocyanin near

the tip/margin of their leaves and on their slightly reduced overall stature (compared with the wild type).

Feeding of ^{14}C -Labeled CO_2

On the day of labeling, the plants received an average of $400 \mu\text{mol m}^{-2} \text{sec}^{-1}$ for 4 hr before feeding began. Two *sed1* plants and one wild-type plant were used in each experiment. For one experiment, the first leaf (L1) of each plant was fed (the average lamina length of L1 from tip to blade joint was 4.7 ± 0.7 cm for *sed1* plants and 5.7 ± 0.1 cm for the wild type). In the other experiment, the tip of the third leaf (L3) was fed on each plant (the average lamina length of L3 from tip to blade joint was 16.4 ± 2.5 cm for *sed1* plants and 19.7 ± 4.9 cm for the wild type). Each of these experiments was replicated. In addition, the base of L3 (lamina length from tip to blade joint was 32.5 cm) from an older *sed1* plant was fed.

Methods of feeding, autoradiography, and scintillation counting were modified from those used in a previous study on sugarcane (Robinson-Beers et al., 1990). Each leaf was clamped into a water-cooled aluminum leaf chamber. Light was supplied to the adaxial surface of the leaf through the glass window in the chamber at an intensity of $550 \mu\text{mol m}^{-2} \text{sec}^{-1}$ with xenon arc lamps. Assimilation of unlabeled CO_2 was monitored using an infrared gas analyzer (model Li-6262; Li-Cor, Inc., Lincoln, NE) until steady state was attained. The leaf was then fed $^{14}\text{CO}_2$ for 1 hr, followed by a 10-min chase with unlabeled CO_2 . Before and after feeding, the rate of photosynthesis was the same (within 10%). The plants were returned to greenhouse conditions for 5 hr, after which they were rapidly dissected. L1 through L5 and the root system of each plant were taped to an 8×10 inch sheet of heavy paper stock.

Under safelights, these preparations were placed into a photographic paper box. A sheet of Kodak SB x-ray film was laid emulsion-side down over the plant material, followed by a sheet of corrugated cardboard. Foam sheets were laid on top of the cardboard to appress the film tightly to the plant parts, after which the boxes were closed and taped shut. These preparations were placed in a freezer at -80°C for 1 week, after which the film was removed and developed.

In addition, samples ($\sim 1 \text{ cm}^2$) of the fed leaf (L1 or L3), the base of an immature sink leaf (L4), and the root system (R) were taken from both wild-type and *sed1* experimental plants (Figures 2A to 2D). As a check to determine whether labeled photosynthate was exported from the fed tip of L3, a 1-cm^2 sample was taken from the base of L3 (Figures 2C and 2D). The tissue samples were placed into scintillation vials containing BioSafe II scintillation cocktail (Research Products International, Mount Prospect, IL). The vials were then gently shaken at $\sim 75 \text{ rpm}$ for 12 hr on a rotary platform shaker. These samples were counted with a liquid scintillation counter (model Ls7800; Beckman Instruments, Fullerton, CA).

Tissue Preparation and Microscopy

Samples were taken from the base, mid-, and tip region of L3 lamina from both *sed1* and wild-type plants. The samples were diced in 50 mM sodium cacodylate buffer, pH 7.1, transferred to vials of fixative consisting of 4% glutaraldehyde, 1% *p*-formaldehyde, and 0.3% Tween 20, and then vacuum infiltrated (~ 190 torr) for 3 hr. After thorough washing in 50 mM cacodylate buffer, the samples were postfixed with 2% osmium tetroxide overnight in a refrigerator. These tissues were dehydrated in a graded acetone series and then embedded in Spurr's epoxy resin (Spurr, 1969).

To describe the anatomical differences between leaves from the two genotypes, thick sections ($\sim 2 \mu\text{m}$) were cut with glass knives and heat-fixed to glass slides. The sections were stained with either 0.05% toluidine blue O or 1% toluidine blue O with 1% borax, depending on the affinity of the material for the stain solution. All tissues were viewed and photographed on an Ultraphot II light microscope (Carl Zeiss, Inc., Thornwood, NY).

For electron microscopy, thin sections (~ 70 to 90 nm) of the above material were cut with a diamond knife (Diatome, Fort Washington, PA) and then lifted on 200-mesh copper grids. These sections were stained first with 3% uranyl acetate in 30% ethanol and then with Reynolds's lead citrate. Thin sections were viewed and photographed with a transmission electron microscope (model JEM 1200-EX; JEOL Corp., Tokyo).

Portions of five mutant leaves and two wild-type leaves were fixed for this work. Twenty sections from each of the sampling regions of each leaf were used for light microscopy. Plasmodesmal ultrastructure was determined by electron microscopic examination of 20 major veins, 50 minor veins, and contiguous tissues of *sed1* plants. Ten major veins, 20 minor veins, and contiguous tissues of wild-type plants were examined.

ACKNOWLEDGMENTS

We thank Dr. Randall Cooraugh, Michael G. Connors, and Bryan R. Ziegler of New Media Center, Division of Information Technology, University of Wisconsin-Madison, for generous use of digital imaging equipment; Drs. Virginia C. Crane and Mark A. Chamberlain at Pioneer Hi-Bred International for helpful discussions; Jennifer R. Gottwald, Christina L. Trivett, James S. Busse, and Tracy L. Saffran for critical review of the manuscript; and Claudia S. Lipke and Kandis Elliot for graphics assistance. This work was supported by National Science Foundation Grant No. IBN-9320218 to R.F.E.

Received November 30, 1995; accepted January 30, 1996.

REFERENCES

- Allison, J.C.S., and Weinmann, H. (1970). Effect of absence of developing grain on carbohydrate content and senescence of maize leaves. *Plant Physiol.* **46**, 435–436.
- Altus, D.P., and Canny, M.J. (1982). Loading of assimilates in wheat leaves. I. The specialization of vein types for separate activities. *Aust. J. Plant Physiol.* **9**, 571–581.
- Beebe, D.U., and Evert, R.F. (1992). Photoassimilate pathway(s) and phloem loading in the leaf of *Moricandia arvensis* (L.) DC. (Brassicaceae). *Int. J. Plant Sci.* **153**, 61–77.
- Bosabalidis, A.M., Evert, R.F., and Russin, W.A. (1994). Ontogeny of the vascular bundles and contiguous tissues in the maize leaf blade. *Am. J. Bot.* **81**, 745–752.
- Botha, C.E.J., and Evert, R.F. (1988). Plasmodesmatal distribution and frequency in vascular bundles and contiguous tissues of the leaf of *Themeda triandra*. *Planta* **173**, 433–441.

- Botha, C.E.J., and van Bel, A.J.E.** (1992). Quantification of symplastic continuity as visualized by plasmodesmograms: Diagnostic value for phloem loading pathways. *Planta* **187**, 359–366.
- Botha, C.E.J., Hartley, B.J., and Cross, R.H.M.** (1993). The ultrastructure and computer-enhanced digital image analysis of plasmodesmata at the Kranz mesophyll-bundle sheath interface of *Themeda triandra* var. *imberbis* (Retz) A. Camus in conventionally fixed leaf blades. *Ann. Bot.* **72**, 255–261.
- Bourquin, S., Bonnemain, J.-L., and Delrot, S.** (1990). Inhibition of loading of ^{14}C assimilates by *p*-chloromercuribenzenesulfonic acid. Localization of the apoplastic pathway in *Vicia faba*. *Plant Physiol.* **92**, 97–102.
- Burnell, J.N.** (1988). An enzymatic method for measuring the molecular weight exclusion limit of plasmodesmata of bundle sheath cells of C_4 plants. *J. Exp. Bot.* **39**, 1575–1580.
- Bush, D.R.** (1993). Proton-coupled sugar and amino acid transporters in plants. *Annu. Rev. Plant Physiol. Plant Mol. Biol.* **44**, 513–542.
- Delrot, S.** (1987). Phloem loading: Apoplastic or symplastic? *Plant Physiol. Biochem.* **25**, 667–676.
- Ding, B., Parthasarathy, M.V., Niklas, K., and Turgeon, R.** (1988). A morphometric analysis of the phloem unloading pathway in developing tobacco leaves. *Planta* **176**, 307–318.
- Ding, B., Haudenschild, J.S., Hull, R.J., Wolf, S., Beachy, R.N., and Lucas, W.J.** (1992). Secondary plasmodesmata are specific sites of localization of the tobacco mosaic virus movement protein in transgenic plants. *Plant Cell* **4**, 915–928.
- Ding, B., Haudenschild, J.S., Willmitzer, L., and Lucas, W.J.** (1993). Correlation between arrested secondary plasmodesmal development and onset of accelerated leaf senescence in yeast acid invertase transgenic tobacco plants. *Plant J.* **4**, 179–189.
- Downton, W.J.S., and Hawker, J.S.** (1973). Enzymes of starch and sucrose metabolism in *Zea mays* leaves. *Phytochemistry* **12**, 1551–1556.
- Eastin, J.A.** (1969). Leaf position and leaf function in corn. Carbon-14 labeled photosynthate distribution in corn in relation to leaf position and leaf function. In *Proceedings of the 24th Annual Corn and Sorghum Research Conference* (Washington, DC: American Seed Trade Association), pp. 81–89.
- Epel, B.L.** (1994). Plasmodesmata: Composition, structure and trafficking. *Plant Mol. Biol.* **26**, 1343–1356.
- Evert, R.F.** (1986). Phloem loading in maize. In *Regulation of Carbon and Nitrogen Reduction and Utilization in Maize*, J.C. Shannon, D.P. Kniewel, and C.D. Boter, eds (New York: American Society of Plant Physiologists), pp. 67–81.
- Evert, R.F., and Russin, W.A.** (1993). Structurally, phloem unloading in the maize leaf cannot be symplastic. *Am. J. Bot.* **80**, 1310–1317.
- Evert, R.F., Eschrich, W., and Heyser, W.** (1977). Distribution and structure of the plasmodesmata in mesophyll and bundle-sheath cells of *Zea mays* L. *Planta* **136**, 77–89.
- Evert, R.F., Eschrich, W., and Heyser, W.** (1978). Leaf structure in relation to solute transport and phloem loading in *Zea mays* L. *Planta* **138**, 279–294.
- Evert, R.F., Botha, C.E.J., and Mierzwa, R.J.** (1985). Free-space marker studies on the leaf of *Zea mays* L. *Protoplasma* **126**, 62–73.
- Evert, R.F., Russin, W.A., and Bosabalidis, A.M.** (1996). Anatomical and ultrastructural changes associated with sink-to-source transition in developing maize leaves. *Int. J. Plant Sci.* **157**, 247–261.
- Fritz, E., Evert, R.F., and Nasse, H.** (1989). Loading and transport of assimilates in different maize leaf bundles. Digital image analysis of ^{14}C -microautoradiographs. *Planta* **178**, 1–9.
- Gamalei, Y.V., van Bel, A.J.E., Pakhomova, M.V., and Sjutkina, A.V.** (1994). Effects of temperature on the conformation of the endoplasmic reticulum and on starch accumulation in leaves with the symplastic minor-vein configuration. *Planta* **194**, 443–453.
- Geiger, D.R.** (1979). Control of partitioning and export of carbon in leaves of higher plants. *Bot. Gaz.* **140**, 241–248.
- Hattersley, P.W., and Browning, A.J.** (1981). Occurrence of the suberized lamella in leaves of grasses of different photosynthetic types. I. In parenchymatous bundle sheaths and PCR (“Kranz”) sheaths. *Protoplasma* **109**, 371–401.
- Heyser, W.** (1980). Phloem loading in the maize leaf. *Ber. Deutsch. Bot. Ges.* **93**, 221–228.
- Hofstra, G., and Nelson, C.D.** (1969). The translocation of photosynthetically assimilated ^{14}C in corn. *Can. J. Bot.* **47**, 1435–1442.
- Jackson, D., Veit, B., and Hake, S.** (1994). Expression of maize *KNOTTED1* related homeobox genes in the shoot apical meristem predicts patterns of morphogenesis in the vegetative shoot. *Development* **120**, 405–413.
- Kalt-Torres, W., Kerr, P.S., Usuda, H., and Huber, S.C.** (1987). Diurnal changes in maize leaf photosynthesis. I. Carbon exchange rate, assimilate export rate, and enzyme activities. *Plant Physiol.* **83**, 283–288.
- Koch, K.E., Tsui, C.-H., Schrader, L.E., and Nelson, O.E.** (1982). Source-sink relations in maize mutants with starch-deficient endosperms. *Plant Physiol.* **70**, 322–325.
- Kutík, J., and Beneš, K.** (1981). The anatomical study of heterotrophic starch formation in leaf segments of maize and pea. *Biol. Plant.* **23**, 52–57.
- Langdale, J.A., and Kidner, C.A.** (1994). *bundle sheath defective*, a mutation that disrupts cellular differentiation in maize leaves. *Development* **120**, 673–681.
- Leisner, S.M., and Turgeon, R.** (1993). Movement of virus and photoassimilate in the phloem: A comparative analysis. *Bioessays* **15**, 741–748.
- Lucas, W.J., Ding, B., and van der Schoot, C.** (1993a). Plasmodesmata and the supracellular nature of plants. *Tansley Review No. 58. New Phytol.* **125**, 435–476.
- Lucas, W.J., Olesinski, A., Hull, R.J., Haudenschild, J.S., Deom, C.M., Beachy, R.N., and Wolf, S.** (1993b). Influence of the tobacco mosaic virus 30-kDa movement protein on carbon metabolism and photosynthate partitioning in transgenic tobacco plants. *Planta* **190**, 88–96.
- Lucas, W.J., Bouché-Pillon, S., Jackson, D.P., Nguyen, L., Baker, L., Ding, B., and Hake, S.** (1995). Selective trafficking of *KNOTTED1* homeodomain protein and its mRNA through plasmodesmata. *Science* **270**, 1980–1983.
- Madore, M.A., Oross, J.W., and Lucas, W.J.** (1986). Symplastic transport in *Ipomea tricolor* source leaves. Demonstration of functional symplastic connections from mesophyll to minor veins by a novel dye-tracer method. *Plant Physiol.* **82**, 432–442.
- Moore, P.J., Fenczik, C.A., Deom, C.M., and Beachy, R.N.** (1992). Developmental changes in plasmodesmata in transgenic tobacco expressing the movement protein of tobacco mosaic virus. *Protoplasma* **170**, 115–127.

- Nelson, O., and Pan, D.** (1995). Starch synthesis in maize endosperms. *Annu. Rev. Plant Physiol. Plant Mol. Biol.* **46**, 475–496.
- Neuffer, M.G., Coe, E.H., and Wessler, S.R.** (1996). Mutants of Maize. (New York: Cold Spring Harbor Laboratory Press), in press.
- Oparka, K.J.** (1993). Signalling via plasmodesmata—The neglected pathway. *Semin. Cell Biol.* **4**, 131–138.
- Oparka, K.J., and Prior, D.A.M.** (1992). Direct evidence for pressure-generated closure of plasmodesmata. *Plant J.* **2**, 741–750.
- Pristupa, N.A.** (1964). Redistribution of radioactive assimilates in the leaf tissues of cereals. *Soviet Plant Physiol.* **11**, 31–36.
- Reismeyer, J.W., Willmitzer, L., and Frommer, W.B.** (1992). Isolation and characterization of a sucrose carrier cDNA from spinach by functional expression in yeast. *EMBO J.* **11**, 4705–4713.
- Reismeyer, J.W., Hirner, L., and Frommer, W.B.** (1993). Potato sucrose transporter expression in minor veins indicates a role in phloem loading. *Plant Cell* **5**, 1591–1598.
- Reismeyer, J.W., Willmitzer, L., and Frommer, W.B.** (1994). Evidence for an essential role of the sucrose transporter in phloem loading and assimilate partitioning. *EMBO J.* **13**, 1–7.
- Rhoads, M.M., and Carvalho, A.** (1944). The function and structure of the parenchyma sheath plastids of the maize leaf. *Bull. Torrey Bot. Club* **71**, 335–346.
- Robinson-Beers, K., Sharkey, T.D., and Evert, R.F.** (1990). Import of ^{14}C -photosynthate by developing leaves of sugar cane. *Bot. Acta* **103**, 424–429.
- Rocher, J.P.** (1988). Comparison of carbohydrate compartmentation in relation to photosynthesis, assimilate export, and growth in a range of maize genotypes. *Aust. J. Plant Physiol.* **15**, 677–686.
- Russell, S.H., and Evert, R.F.** (1985). Leaf vasculature in *Zea mays* L. *Planta* **164**, 448–458.
- Sonnenwald, U., Lerchl, J., Zrenner, R., and Frommer, W.** (1994). Manipulation of sink-source relations in transgenic plants. *Plant Cell Environ.* **17**, 649–658.
- Spurr, A.R.** (1969). A low-viscosity epoxy resin embedding medium for electron microscopy. *J. Ultrastruct. Res.* **26**, 31–43.
- Stitt, M., and Sonnenwald, U.** (1995). Regulation of metabolism in transgenic plants. *Annu. Rev. Plant Physiol. Plant Mol. Biol.* **46**, 341–368.
- Thiagarajah, M.R., Hunt, L.A., and Mahon, J.D.** (1981). Effects of position and age on leaf photosynthesis in maize (*Zea mays*). *Can. J. Bot.* **59**, 28–33.
- Tollenaar, M., and Daynard, T.B.** (1982). Effect of source-sink ratio on dry matter accumulation and leaf senescence in maize. *Can. J. Plant Sci.* **62**, 855–860.
- Tucker, E.B.** (1993). Azide treatment enhances cell-to-cell diffusion in staminal hairs of *Setcreasea purpurea*. *Protoplasma* **174**, 45–49.
- Tucker, E.B., and Tucker, J.E.** (1993). Cell-to-cell selectivity in staminal hairs of *Setcreasea purpurea*. *Protoplasma* **174**, 36–44.
- Turgeon, R.** (1989). The sink-source transition in leaves. *Annu. Rev. Plant Physiol. Plant Mol. Biol.* **40**, 119–138.
- Turgeon, R., and Beebe, D.U.** (1991). The evidence for symplastic phloem loading. *Plant Physiol.* **96**, 349–354.
- Valle, E.M., Craig, S., Hatch, M.D., and Heldt, H.W.** (1989). Permeability and ultrastructure of bundle sheath cells isolated from C_4 plants: Structure-function studies and the role of plasmodesmata. *Bot. Acta* **102**, 276–282.
- van Bel, A.J.E.** (1987). The apoplast concept of phloem loading has no universal validity. *Plant Physiol. Biochem.* **25**, 677–686.
- van Bel, A.J.E.** (1993). Strategies of phloem loading. *Annu. Rev. Plant Physiol. Plant Mol. Biol.* **44**, 253–281.
- van Bel, A.J.E., van Kesteren, W.J.P., and Papenhuijzen, C.** (1988). Ultrastructural indications for coexistence of symplastic and apoplastic phloem loading in *Commelina benghalensis* leaves. *Planta* **176**, 159–172.
- Wagmann, E., and Zambryski, P.** (1994). Gateways for rapid information transfer. *Curr. Biol.* **4**, 713–716.
- Wagmann, E., and Zambryski, P.** (1995). Tobacco mosaic virus movement protein-mediated protein transport between trichome cells. *Plant Cell* **7**, 2069–2079.
- Wardlaw, I.F.** (1990). The control of carbon partitioning in plants. *Tansley Review No. 27. New Phytol.* **116**, 341–381.
- Weiner, H., Burnell, J.N., Woodrow, I.E., Heldt, H.W., and Hatch, M.D.** (1988). Metabolite diffusion into bundle sheath cells from C_4 plants. Relation to C_4 photosynthesis and plasmodesmatal function. *Plant Physiol.* **88**, 815–822.
- Wolf, S., Deom, C.M., Beachy, R.N., and Lucas, W.J.** (1989). Movement protein of tobacco mosaic virus modifies plasmodesmatal size exclusion limit. *Science* **246**, 377–379.
- Wyse, R.E.** (1986). Sinks as determinants of assimilate partitioning: Possible sites for regulation. In *Phloem Transport*, J. Cronshaw, W.J. Lucas, and R.T. Giaquinta, eds (New York: Alan R. Liss, Inc.), pp. 197–209.

NOTE ADDED IN PROOF

While this article was in proof, *sed1* was published as the acronym for a *senescence diminished* mutant of maize. Therefore, we will retain *sucrose export defective1* as the name for this mutant but will use the acronym *sxd1* in all further work. We thank Dr. Ed Coe (University of Missouri) for his help in selecting and approving *sxd1* as the appropriate designation.